Journal of Magnetism and Magnetic Materials 355 (2014) 254–258

Contents lists available at ScienceDirect

Journal of Magnetism and Magnetic Materials

journal homepage: www.elsevier.com/locate/jmmm

The effects of the iron content on structural and magnetic properties of $Sr_{0.80}La_{0.20}Fe_xZn_{0.15}O_{19}$ hexagonal ferrites

Yujie Yang, Xiansong Liu*, Dali Jin, Kai Huang, Shang Gao

Engineering Technology Research Center of Magnetic Materials, School of Physics & Materials Science, Anhui University, Hefei 230601, Anhui, PR China

ARTICLE INFO

Article history:
Received 5 September 2013
Received in revised form
30 November 2013
Available online 22 December 2013

Keywords:
Hexagonal ferrites
Iron content
La–Zn substitution
Magnetic properties
X-ray diffraction

ABSTRACT

The hexagonal ferrite $Sr_{0.80}La_{0.20}Fe_xZn_{0.15}O_{19}$ ($10.65 \le x \le 12.05$) magnetic powder and magnets were synthesized by the ceramics process. The phase components of the hexagonal ferrite magnetic powder were studied using X-ray diffraction (XRD). Scanning electron microscopy (SEM) was used to investigate the morphology of the sintered magnets. The effects of the iron content on magnetic properties of the magnets were studied systematically. The remanence (B_r) and maximum energy product [$(BH)_{max}$] for the magnets at $x=11.25$ reached the maximum value of 414.5 mT and 32.24 kJ/m^3, respectively. The intrinsic coercivity (H_{cj}) and magnetic induction coercivity (H_{cb}) for the magnets at $x=11.65$ reached the maximum value of 265.8 kA/m and 257.8 kA/m, respectively.

1. Introduction

The hexagonal ferrites are ceramic magnetic materials and have played an important role in many technological and industrial fields. Among various hexagonal ferrites, the M-type hexagonal ferrites have been widely used as permanent magnets, microwave devices, magneto-optics and magnetic recording media due to a low cost, outstanding chemical stability and large uniaxial magnetocrystalline anisotropy [1,2]. In order to fulfill various applications, many attempts have been made to improve the magnetic properties of M-type hexagonal ferrites by adding or doping some elements. La^{3+} substitution of Sr^{2+} and substitution of transition metals such as Zn^{2+}, Co^{2+}, Mn^{2+}, Ni^{2+}, Ti^{2+} and Ti^{4+} on the Fe^{3+} have been investigated [3–6]. On the other hand, M-type hexagonal ferrites with combined substitution such as La–Co, La–Zn, La–Cu, Co–Ti, and so on, were synthesized by sol–gel, rf diode sputtering or ceramic methods [7–15].

Partial substitution of Ba^{2+}–Fe^{3+} or Sr^{2+}–Fe^{3+} by La^{3+}–Zn^{2+} ions in M-type ferrites can lead to a change of the intrinsic magnetic properties [9–13]. Corral-Huacuz et al. prepared the La–Zn substituted barium ferrite powders by sol–gel and found out that La–Zn substitution could increase the saturation magnetization and yield a more homogeneous microstructure and finer crystallite sizes [9]. Shen et al. prepared the La–Zn substituted strontium ferrite nanofibers by sol–gel and reported that a small amount of La–Zn substitution could increase the saturation magnetization and lead to a continuous reduction of the coercivity with the increase of La–Zn substitution [11]. Liu et al. synthesized the La–Zn substituted strontium ferrite thin films and pointed out that a proper amount of La–Zn substitution could improve the saturation magnetization [12]. However, no prior studies were carried out to investigate the La–Zn substituted hexagonal ferrites with different iron contents prepared by the ceramics process.

In this paper, the hexagonal ferrite $Sr_{0.80}La_{0.20}Fe_xZn_{0.15}O_{19}$ ($10.65 \le x \le 12.05$) magnetic powder and magnets were synthesized according to the ceramics process. The effects of the iron content on the structure and magnetic properties of hexagonal ferrites $Sr_{0.80}La_{0.20}Fe_xZn_{0.15}O_{19}$ have been studied systematically.

2. Experimental procedure

The samples of hexagonal ferrite $Sr_{0.80}La_{0.20}Fe_xZn_{0.15}O_{19}$ magnetic powder and magnets were obtained using the ceramics process. Raw materials used in the present study were $SrCO_3$ (97% purity), La_2O_3 (99% purity), Fe_2O_3 (98% purity) and ZnO (99% purity). The raw materials were weighed in the nominal ratio in a stoichiometric composition of $Sr_{0.80}La_{0.20}Fe_xZn_{0.15}O_{19}$, where x varies from 10.65 to 12.05 with about 0.2 increment. Mixtures of these raw materials were milled in water for 6 h with an angular velocity of 80 rpm and a ball-to-power weight ratio of 12:1. The milling processes were performed in ball mill using hardened steel balls with diameter of 8 mm. The mixed power was dried, crushed, and sifted. These samples were made into balls of about Φ 8 mm, and the temperature was increased up to 1250 °C in a muffle; and then these balls were calcined for 2 h in air. The calcined samples

* Corresponding author. Tel./fax: +86 551 65107674.
E-mail address: xiansongliu@ahu.edu.cn (X. Liu).

0304-8853/$ - see front matter © 2013 Elsevier B.V. All rights reserved.
http://dx.doi.org/10.1016/j.jmmm.2013.12.010

were shattered to particles less than 100 μm using a vibration mill, then wet-milled with additives ($CaCO_3$, $SrCO_3$, SiO_2, Cr_2O_3, Al_2O_3 or H_3BO_3) for 13 h by using a ball-mill. The finely milled slurry with a diameter of about 0.75 μm was pressed into green pellets with Φ 30 × 15 mm under 310 MPa in the magnetic field of 900 kA/m, which was parallel to the pressing direction. The green pellets were sintered in a muffle at 1190 °C for 1.5 h in air.

The X-ray diffraction (XRD) patterns were collected on a PANalytical X′Pert Pro diffractometer in continuous mode using Cu K_α radiation. The morphology of the sintered samples was observed by a HITACHI S-4800 scanning electron microscopy (SEM). The magnetic properties of the sintered magnets were measured using a magnetometer (Model MATS-2000, National Institute of Metrology of China).

3. Results and discussion

3.1. Microstructure

Fig. 1 shows the X-ray diffraction patterns for the hexagonal ferrite $Sr_{0.80}La_{0.20}Fe_xZn_{0.15}O_{19}$ magnetic powder with different iron contents (x) from 10.65 to 11.25. Fig. 2 displays the X-ray diffraction patterns for the hexagonal ferrite $Sr_{0.80}La_{0.20}Fe_xZn_{0.15}O_{19}$ magnetic powder with different iron contents (x) from 11.45 to 11.65. As can be seen from Figs. 1 and 2, there is only the magnetoplumbite phase in the $Sr_{0.80}La_{0.20}Fe_xZn_{0.15}O_{19}$ magnetic powder with the iron content (x) from 10.65 to 11.65, which means that La^{3+} and Zn^{2+} ions enter the magnetoplumbite lattice without second phases. However, as x increases to 11.85, another phase of hematite (α-Fe_2O_3) begins to occur, and the amount of hematite (α-Fe_2O_3) increases with increase in the iron content (x). It is found

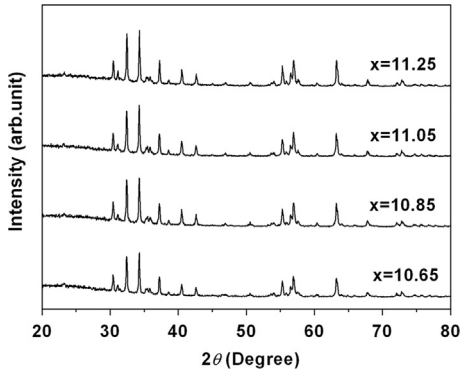

Fig. 1. X-ray diffraction patterns for the hexagonal ferrite $Sr_{0.80}La_{0.20}Fe_xZn_{0.15}O_{19}$ magnetic powder with different iron content (x) from 10.65 to 11.25.

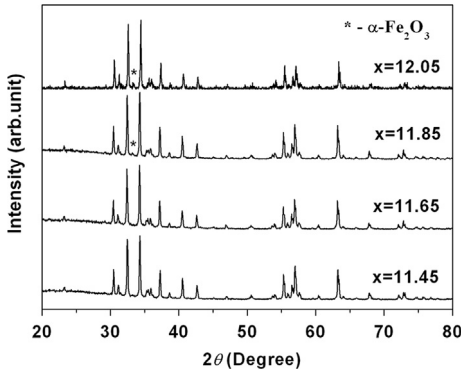

Fig. 2. X-ray diffraction patterns for the hexagonal ferrite $Sr_{0.80}La_{0.20}Fe_xZn_{0.15}O_{19}$ magnetic powder with different iron content (x) from 11.45 to 12.05.

that the intensity of the magnetoplumbite phase becomes higher as x is increased from 10.65 to 12.05. It can be concluded that the iron content (x) plays an important role in the formation of the single-phase hexagonal ferrite, for which the iron content (x) is smaller than that of the stoichiometric [16]. The results are in agreement with those reported by Wang et al. [17].

The lattice constants (a) and (c) are calculated from the value of the interplanar spacing d_{hkl} corresponding to (107) peaks and (114) peaks according to the following equation which characterizes the relationship between d_{hkl} and the lattice constants (a) and (c):

$$d_{hkl} = \left(\frac{4}{3}\frac{h^2+hk+k^2}{a^2}+\frac{l^2}{c^2}\right)^{-1/2}$$

Table 1 indicates the lattice constants (a) and (c) of the hexagonal ferrite $Sr_{0.80}La_{0.20}Fe_xZn_{0.15}O_{19}$ magnetic powder with different iron contents (x) from 10.65 to 12.05. As shown in Table 1, the lattice constant (c) of the magnetic power fluctuates with the iron content (x), at x=11.65 it reaches the maximum value 23.0125 Å and at x=12.05 it reaches the minimum value 22.9646 Å. And a similar trend is observed for the lattice constant (a). Compared with the lattice constant (c), the change in the lattice constant (a) is not substantial in the iron content range. The change of crystal axis ratios of c/a with different iron contents (x) from 10.65 to 12.05 is shown in Fig. 3. It can be seen from Fig. 3 that the crystal axis ratios of c/a are basically the same. According to Verstegen and Stevels, an examination of c/a parameter ratio may quantify the structure type, as the M-type structure can be assumed if the ratio is observed to be lower than 3.98 [18]. The crystal axis ratios of c/a for the magnets range from 3.9140 to 3.9189, which are well within the ratio range of M-type structures.

Fig. 4 shows two typical SEM micrographs of the hexagonal ferrite $Sr_{0.80}La_{0.20}Fe_xZn_{0.15}O_{19}$ with the iron content (x) of 11.25. Fig. 4(a) indicates the micrograph perpendicular to the pressing direction. As can be seen from Fig. 4(a), the hexagonal ferrite magnet has formed the perfect hexagonal structure and the particles are distributed evenly. Fig. 4(b) indicates the micrograph

Table 1
Lattice constants (a) and (c) for the hexagonal ferrite $Sr_{0.80}La_{0.20}Fe_xZn_{0.15}O_{19}$ magnetic powder with different iron contents (x) from 10.65 to 12.05.

Iron content (x)	c (10^{-10} m)	a (10^{-10} m)
10.65	23.0095	5.8743
10.85	22.9920	5.8670
11.05	23.0045	5.8752
11.25	22.9914	5.8724
11.45	22.9742	5.8685
11.65	23.0125	5.8761
11.85	22.9898	5.8720
12.05	22.9646	5.8693

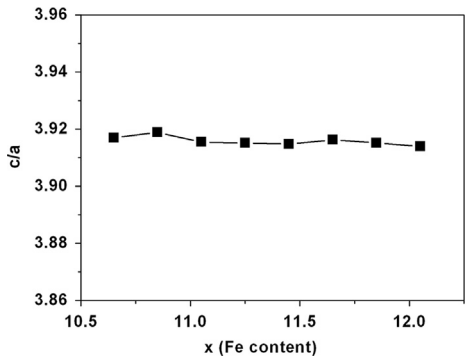

Fig. 3. Crystal axis ratio of c/a with different iron content (x) from 10.65 to 12.05.